N75 28839

SLOW-SCAN OPERATION OF LONG LINEAR CCD ARRAYS

Michael Vicars-Harris
Fairchild Space and Defense Systems
Syosset, New York

The performance and characteristics of Fairchild long linear CCD arrays present a unique design input to slow-scan imaging systems. Slow-scan imaging generally results from requirements for either very high resolution or for very long integration times, or both. Linear CCD arrays used singly or in optically butted assemblies permit practical implementation of long line array systems with 6000 or more picture elements per line with readout rates in excess of 5 MHz. Display and tape recording of slow-scan imagery with over 1000 picture elements per line also presents unique challenges. This paper discusses performance results and the operation of the Fairchild 1728-element CCD arrays for generation of high-resolution slow-scan imagery and some approaches for recording and display of the imagery. The implication of dark current and its control is discussed.

I. INTRODUCTION

Current CCD technology is limited to area arrays no larger than approximately 500 X 400 photo sensors. For system applications which require higher-resolution imagery, CCD linear arrays provide a practical solution.

The Fairchild 1728-element CCD linear array is a two-phase buried-channel device with 1728 photo elements on a 13-μm pitch (Ref. 1). Readout registers and video amplifier are included on the chip, and the device offers wide dynamic range. A summary of measured performance of this array is given in this paper, together with a review of some system applications and parameters.

"Slow-scan" operation is defined in this case as operation at frame rates much less than 30 frames per second. This includes both high-resolution slow-scan security systems, in which sequential frames are panned at a slow rate, and "push-broom" type cameras, in which the array is contained in a moving vehicle and is used to scan a continuous strip. The latter approach would cover wide-angle high-resolution strip reconnaissance cameras, multi-spectral earth resources systems, and environmental monitoring systems.

II. MEASURED PERFORMANCE OF 1728-ELEMENT ARRAYS

Figure 1a shows the typical signal transfer characteristics for a CCLID-1728, with the array output voltage in mV plotted against exposure in $\mu J/m^2$. Saturation for this array occurred at approximately 160 mV, at which point responsivity becomes nonlinear, with blooming occurring at about 180 mV.

Table 1a gives average results of characterization tests of 1728-element arrays at room temperature and at -20°C. As expected from theory, dark current (I_D) approximately halves for every 10°C reduction in chip temperature over this range, while parameters such as responsivity are essentially unchanged.

Spectral response is shown in Figure 1b for two devices from the same wafer. The photosensors on the 1728 arrays are covered by a transparent polysilicon electrode with a silicon dioxide insulator. These layers produce interference patterns in the incident light which result in the peaks and valleys that are seen in these response curves. These are dependent upon the relative thickness of the layers and also the angle of incidence of the rays. Quantum efficiencies of 10%, 30%, and 60% are shown on the same figure for reference purposes.

Figure 2 shows the combined MTF curves for a CCD 1728 array and a B & L Super Baltar 3-in. f/2 lens, measured at four different bands. At the array limiting resolution of 38.5 lp/mm, the MTF is 38% in the band 0.5 - 0.6 µm, 35% in the band 0.6 - 0.7 µm, 23% in the band 0.7 - 0.8 µm, and 18% in the band 0.8 - 1.1 µm. Measurement of the wideband MTF is limited by the ability of the lens to focus simultaneously over the full silicon response of the array.

Transfer inefficiency was measured at 1 MHz both at room temperature and at -20°C. Transfer inefficiency in the readout register results in some charge being left behind after each clock transfer, and this can result in smearing of the information which is being read out as well as in degradation of MTF. Measurements were made using a light spot 5 μm in diameter to image onto one photosensor. The amplitude of the output signal and the trailing pulse signal were measured from each end of the array. The range of transfer efficiencies for all devices was between 0.99995 and 0.99998 per transfer for both temperatures. The effect on MTF for $\eta = 0.99998$ would be to reduce an MTF of 40% for the first elements read out to 38.6% at the opposite end of the array; i.e., the effect on MTF is negligible with these efficiencies.

Crosstalk was measured using the same light probe as in the transfer inefficiency measurements. Results are shown in Table 1b. As expected, crosstalk rises with increasing wavelength because of the deeper penetration of photons at longer wavelengths.

On the 1728 devices, signal charge is integrated in the photo elements during a line integration, then transferred in parallel from the photosensor to the readout registers. If all of this charge is not transferred, there will be a residual image. The efficiency of this transfer is a function of transfer time. Typically this should exceed 1 μs, and if a 10-μs transfer pulse is used, residual image will be negligible.

III. SYSTEM APPLICATIONS

Several slow-scan cameras have been built at Fairchild Space and Defense Systems using 1728-element arrays. For a typical camera which generates a 1728 X 1728 element picture in 4 seconds, the total power required is under 2 1/2 watts and the camera volume is under 20 cubic inches, excluding the lens. In some of these cameras, provision was made for array cooling using a thermoelectric cooler underneath the CCD array. Cooling of an array is only beneficial when the noise equivalent exposure for the system is being limited by dark current noise (Ref. 2).

Dark current noise falls into two categories, temporal and coherent. Temporal noise is random and results from the average I_D for the device, which is of course temperature-dependent. Coherent noise is defined in this instance as the dark current signature which results from the nonuniform dark signal generation from photosensor to photosensor. Variation across an array can be up to ±50% of I_D. At signal levels approaching the noise equivalent exposure, this signature appears as striation across the image in the direction of mechanical scan or motion. Though this coherent noise can be cosmetically objectionable, a useful signal which is below this level can still be extracted.

In a typical application, where the CCD array temperature could exceed 45° C and an integration period of more than 2 milliseconds per line is required, cooling is accomplished using a thermoelectric device (TED). A 1-watt, single-stage TED which is only slightly larger than the CCD package (24 pin DIP) provides a temperature depression of approximately 25° C between the chip and ambient.

A larger temperature depression, approximately 40° C, has been achieved using a 4-watt TED. In this case, care is required to thermally isolate the CDD package from losses through the DIP pins to the printed card, and to adjacent components. Also, in this case chip dissipation is held to under 100 mW total. At low clock frequencies, chip dissipation is determined principally by the I^2R losses of the on-chip amplifier, which is of the order of 50 mW. Power dissipation P due to clocking can be determined from the formula $P = CV_c^2 fc$, where C is the total capacitance of the clocking gates, V_c is the clock voltage amplitude, and fc is the clock frequency. Typically $P \approx 30$ mW at 1 MHz.

For "push-broom" applications requiring very high resolution, many thousands of picture elements are required in a single line. For these situations, optical butting of several arrays can be achieved. One approach, which uses a beam splitting prism to optically align three arrays, is shown in Figure 3. Longer scanners are practical because of the high geometric accuracy of the arrays. For an array with a photosensor pitch of 13 μm, accuracy is better than ±0.2 μm, noncumulative, and the optical alignment between arrays can be made better than ±10 μm. Data reduction techniques can be applied to reduce the effect of the signatures of the arrays, which are caused by small variations in responsivity and transfer characteristics, since these are stable and repeatable for any one device. Thus they can be predetermined for each device used in the scanner. No abnormal characteristics have been observed for the end elements on any device; therefore, optical butting can be contiguous and does not require any overlap or combining of photo elements.

IV. VIDEO RECORDING AND DISPLAY

For a single 1728 array operating at clock rates up to 2 MHz, data has been stored successfully using a standard Sony rotating head video recorder. In this case, the recorder will make several head rotations for each 1728 X 1728 frame, and requires insertion of a pseudo sync pulse after each head rotation to maintain synchronism. Figure 4 shows a recording made with a 1728-line scanning camera, which was then played back using a slow-scan electrostatically deflected CRT display. In this particular example, detailed analysis of the recorded picture was made possible by playing one slow-scan frame, or portion of a frame, into a scan converter operating at a 30 frame per second output. Since even the best monitors start to degrade resolution at over 1000 lines, it is important to be able to expand selected portions of the frame for viewing at full resolution.

When multiple arrays are used simultaneously, the video output requires more complex mass data storage techniques. For instance, for ten 1728 arrays simultaneously being clocked at 5 MHz, the video bandwidth will be 1/2 X 50 MHz, i.e., one half of the fundamental clock frequency. Storage and display of video at a 25-MHz bandwidth clearly require special equipment for both recording and display. Real-time viewing of the total scene can be done at a lower resolution, with detailed analysis performed by either electronically "zooming" in on the area of interest, or by transferring the recording to film.

V. CONCLUSION

Systems configured around the 1728-element CCD array have been successfully built and demonstrated in Fairchild Syosset. A brief summary has been given in this paper. All of these systems share the advantage inherent in the use of CCDs of having low power consumption, small size, high metricity, and a wide operating dynamic range.

ACKNOWLEDGEMENT

The author would like to thank the many people who were involved in these programs, and in particular I. Hirschberg for many useful discussions, and A. Green and F. Moy for performance data and testing.

REFERENCES

1. C. K. Kim, "Two-Phase Charge Coupled Linear-Imaging Devices with Self Aligned Implanted Barrier," IEDM Technical Digest, Dec. 1974, p. 55.

2. C. K. Kim and R. H. Dyck, "Low Light Level Imaging with Buried Channel Charge Coupled Devices," Proc. IEEE, Aug. 1973, p. 1146.

Table 1. Measured performance characteristics of CCLID 1728 arrays (clock frequency = 1 MHz, integration time = 1.8 ms)

(a) General characteristics

AVERAGE VALUES	TRANS. EFF. η	DARK CURRENT		SAT. EXPOSURE $\mu J/M^2$	NEE $\mu J/M^2$	DYNAMIC RANGE	RESPONSIVITY-mA/W				
		I_D nA	NON-UNIFORM % I_D				.5-.6	.6-.7	.7-.8	.8-1.1	2854°K .4–1.2
AT +25°C	.99995	2	±25	2060	1.5	1441	171	254	304	180	156
AT -20°C	.99995	.1	–	2060	1.5	1441	–	–	–	–	156

(b) Element-to-element crosstalk

IRRADIANCE BANDPASS μM	CROSSTALK (%)			
	ADJACENT ELEMENT	2 ELEMENTS AWAY	3 ELEMENTS AWAY	4 ELEMENTS AWAY
.5 TO .6	5%	0	0	0
.6 TO .7	7%	1%	0	0
.7 TO .8	12%	2%	1%	0
.8 TO 1.1	21%	7%	3%	1%

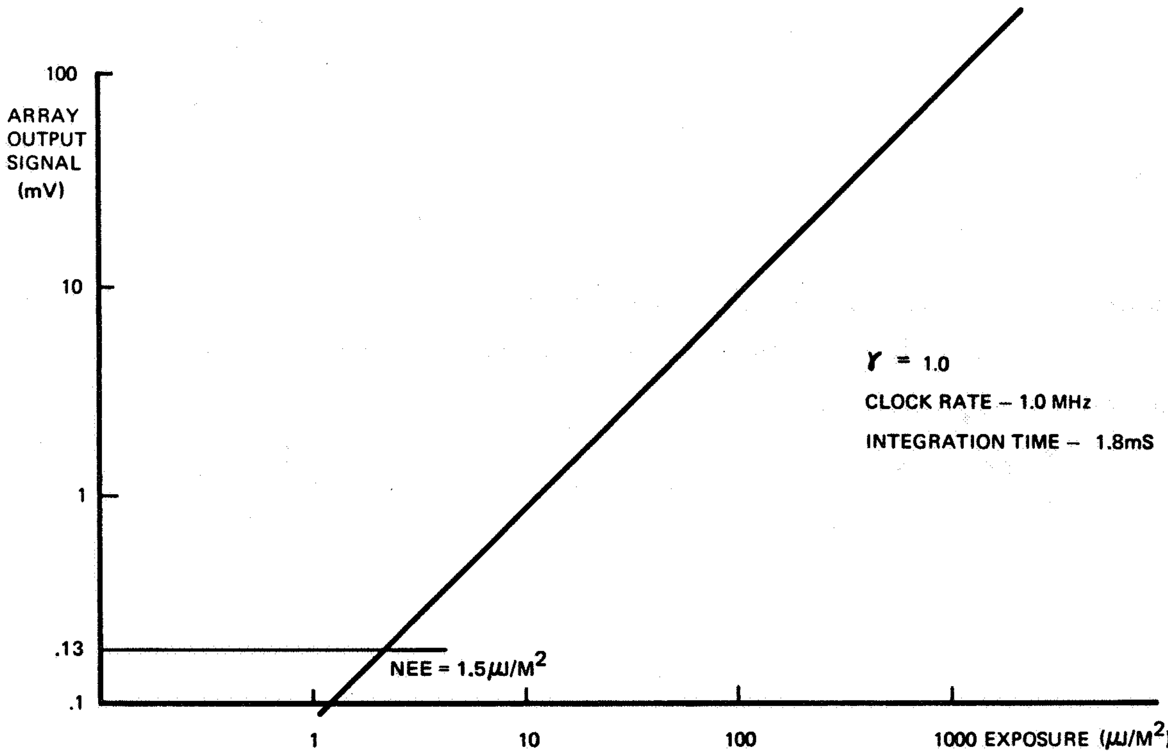

Figure 1a. Signal transfer curve

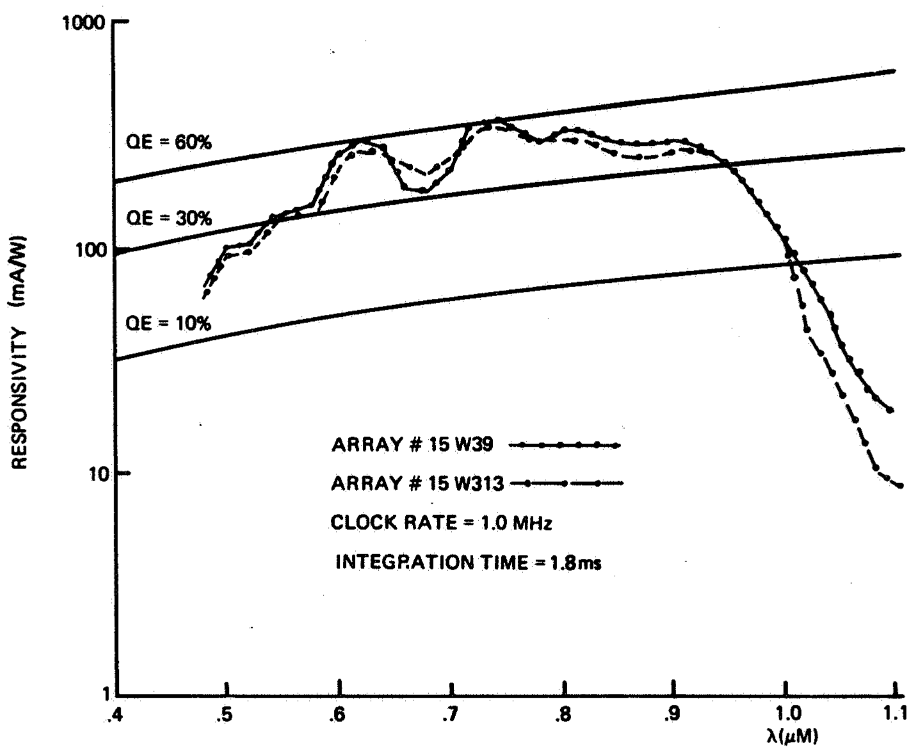

Figure 1b. Spectral response of two arrays from the same wafer

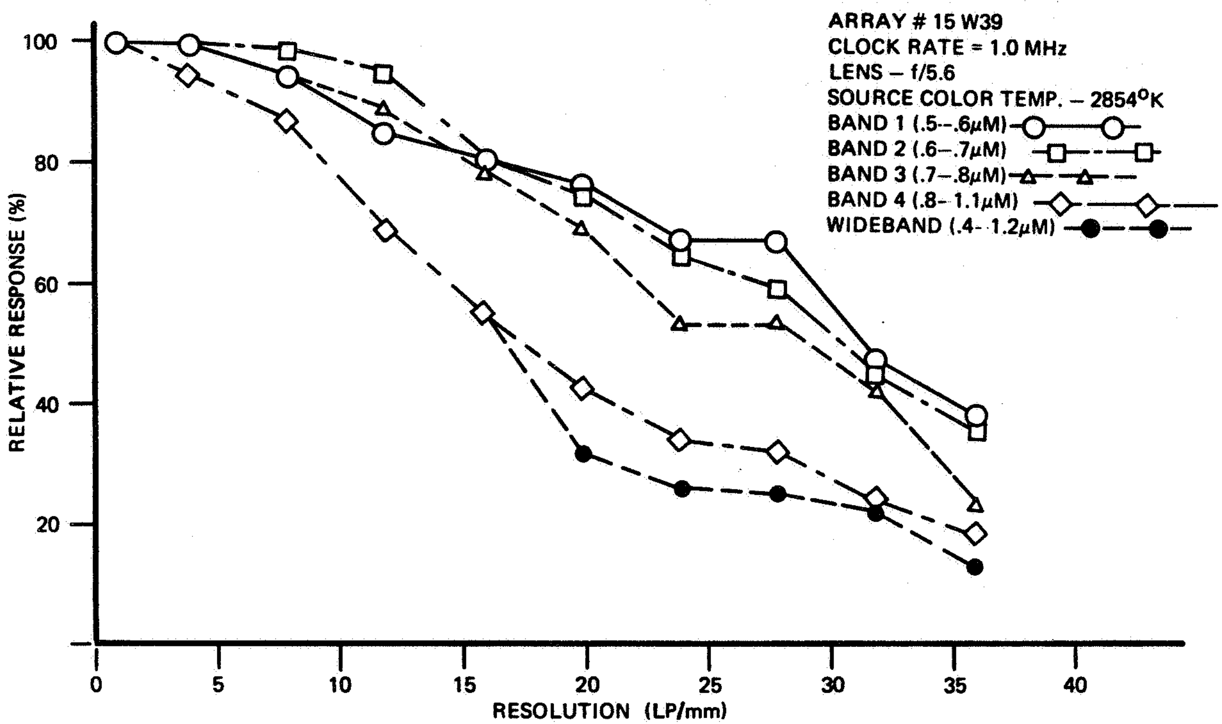

Figure 2. Squarewave response -- in phase

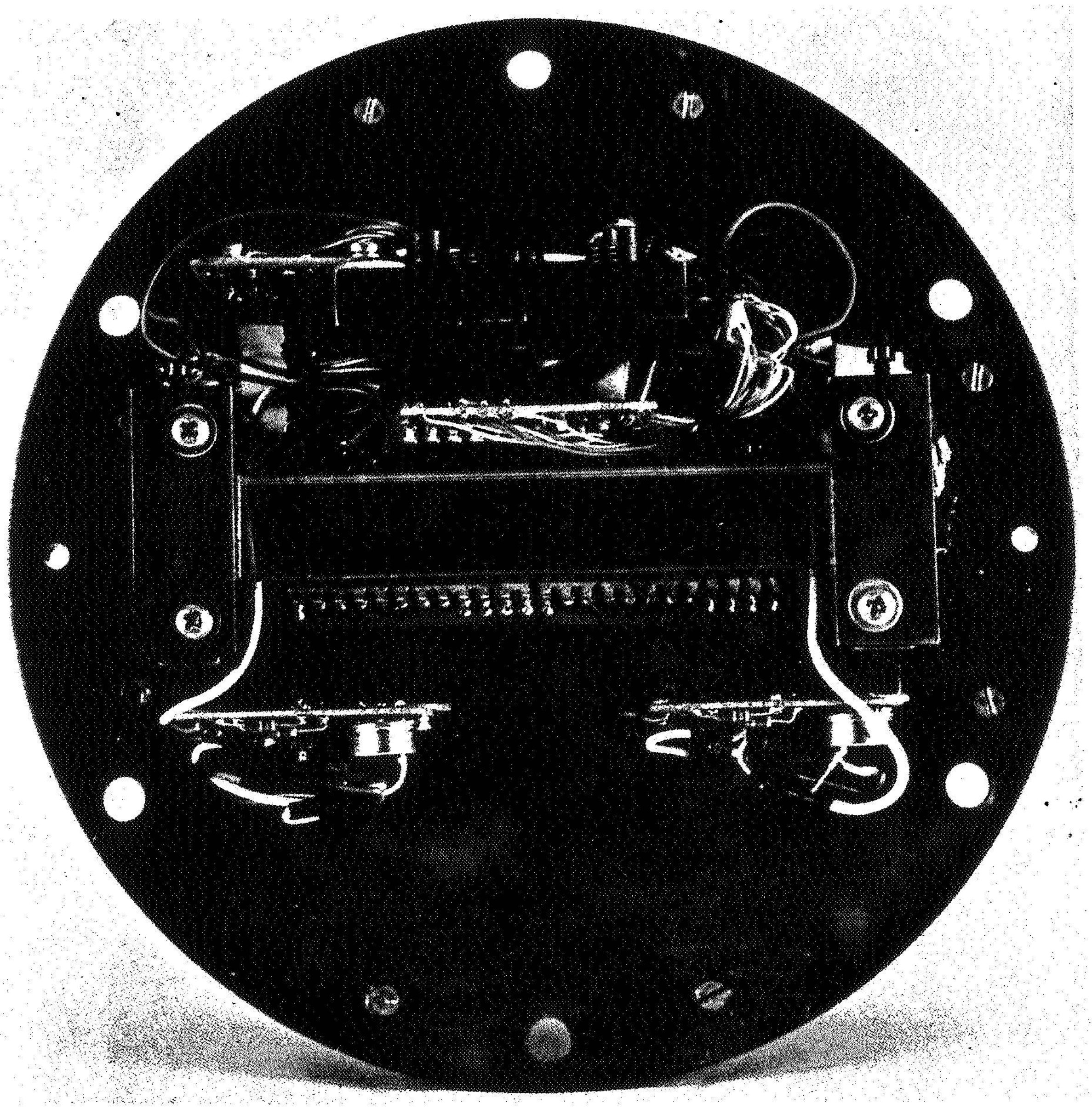

Figure 3. EWACS optical butting assembly

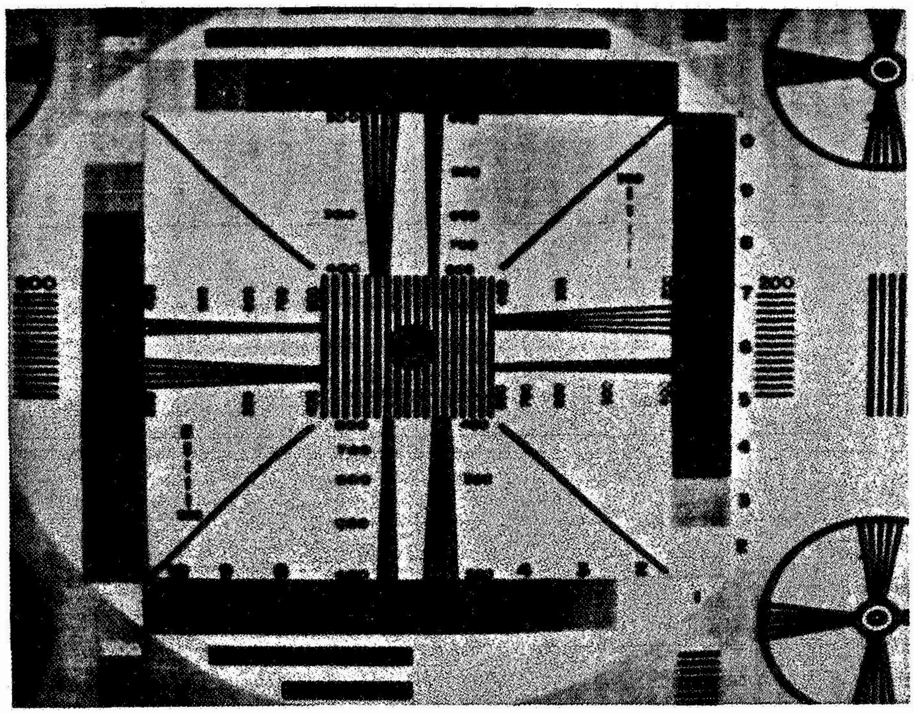

Figure 4a. Camera output image

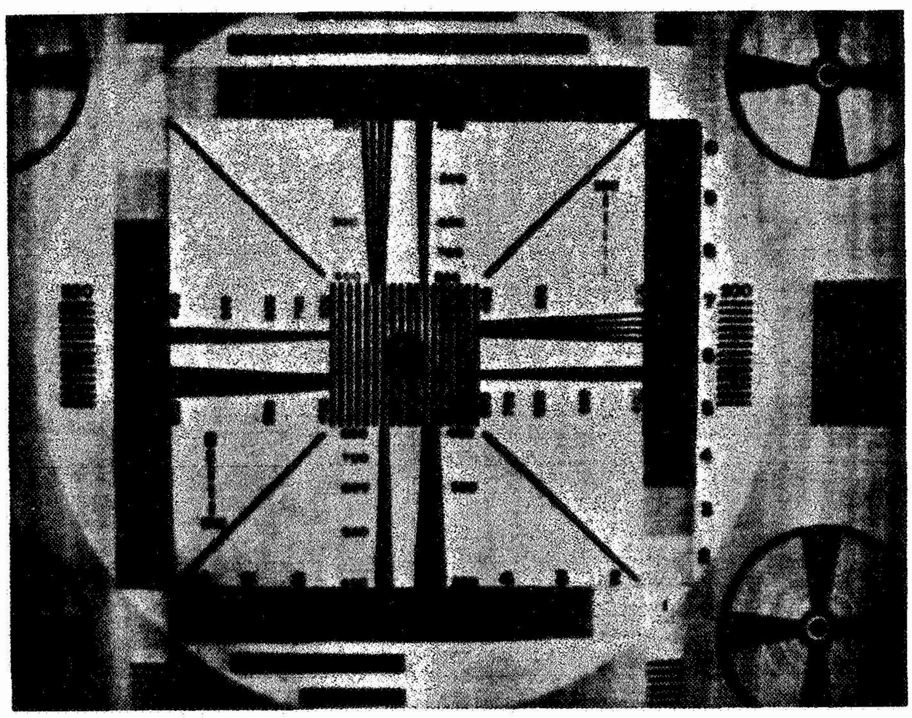

Figure 4b. Tape recorder output image